CHAPTER IV

RESULTS

4.1 The functional relationship between iron, glycogen synthase kinase-3β, microglial activation and its neurotoxicity

4.1.1 Effects of iron and LiCl on the inhibitory phosphorylation of GSK-3β during microglial activation

Because *in vivo* under pathological conditions activated microglia has been shown to be enriched for iron (Connor *et al.*, 1992a; Berg *et al.*, 2001), therefore iron supplemented and lipopolysaccharide (LPS)-stimulated cultures of BV2 microglia was developed to mimic progressive iron accumulation by activated microglia and used this model to address the role of iron in microglial activation, specifically mediated by GSK-3β in an established murine BV2 microglial cell line. The activity of GSK-3β was determined by the measurement phosphorylation of GSK-3β at Ser9, a critical site known for inhibit its activity. In this set of experiments, BV2 microglia were also treated with GSK-3β inhibitor, Lithium chloride (LiCl) to confirm the involvement of GSK-3β in microglial activation. After 1 hr of treatments, total cell lysates were first immunoblotted with anti-phospho-Ser9-GSK-3β followed by anti-total-GSK-3β monoclonal antibodies. The levels of phospho-Ser9-GSK-3β were compared to that of total GSK-3β. As shown in Figure 4.1, the presence of iron alone in the cell culture medium significantly decreased phosphor-Ser9-GSK-3β levels in untreated BV2 microglia in a dose-dependent manner. Exposing BV2 microglia to LPS significantly decreased phosphor-Ser9-GSK-3β levels compared to that of untreated control. If iron was presented in the cell culture medium while the cells were activated by LPS, the levels of phosphor-Ser9-GSK-3β markedly decreased in a dose-dependent manner. LiCl, on the other hand, significantly increased phospho-Ser9-GSK-3β levels in untreated BV2 microglia. Treatment with LiCl also significantly increased phospho-Ser9-GSK-3β levels in LPS-activated BV2 cells and this effect was observed even in

the presence of iron in the cell culture medium. These results demonstrated that iron increased GSK-3β activity in microglia by decreasing the levels of inhibitory phosphorylation of GSK-3β at Ser-9.

4.1.2 Effects of iron and LiCl on NF-κB nuclear translocation

The downstream targets of GSK-3β are included NF-κB, a known transcription factor involved in microglial activation and inflammation. Previous experiment the result was shown that iron increased GSK-3β activity in LPS-activated BV2 microglia. It was hypothesized that iron might regulate GSK-3β activity leading to alter nuclear translocation of NF-κB in LPS-activated BV2 microglia. Therefore, the next study to investigate the role of iron on nuclear translocation of NF-κB and ask whether inhibition of GSK-3β by LiCl in the presence or absence of iron would decrease the nuclear translocation of NF-κB. In this experiment, the levels of the NF-κB p65 subunit in the nuclei of LPS-treated cultures of BV2 microglia were determined by immunofluorescence staining and ELISA assays. As shown in Figure 4.2A, immunofluorescence microscopy revealed that NF-κB p65 were mainly localized to the cytoplasm of untreated cultures of BV2 microglia. Exposing BV2 microglia to LPS increased the nuclear localization of NF-κB p65. The levels of NF-κB p65 in the nuclei of LPS-treated cultures of BV2 microglia were further increased if iron was presented in the cell culture medium. Inhibiting GSK-3β by LiCl blocked LPS-induced NF-κB p65 nuclear translocation and this inhibitory effect was observed even in the presence of iron in the cell culture medium. Consistent with the results from immunofluorescence staining assay, similar data was obtained by NF-κB p65 ELISA assay, in which the concentrations of NF-κB p65 in the nuclear extracts prepared from parallel cultures were determined and were shown in Figure 4.2B. These results demonstrate that the nuclear translocation of NF-κB in LPS-activated BV2 microglia is linked to GSK-3β signaling cascade, which propose to be regulated by iron. These results were also in line with the findings that the presence of iron in the cell culture

medium of untreated or LPS-treated BV2 microglia associated with a further increase in GSK-3β activity and LiCl treatment even in the presence of iron decrease GSK-3β activation.

4.1.3 Effects of iron and LiCl on the production of inflammatory mediators, markers of microglial activation

Previous experiment the results were demonstrated that iron increased GSK-3β activity and nuclear translocation of NF-κB in LPS-activated BV2 microglia. Since NF-κB is a key transcription factor that regulate the expression of many inflammatory mediators, markers of microglial activation including MMP-9, TNF-α, IL-1β and NO. Therefore, it was hypothesized that the production of MMP-9, TNF-α, IL-1β and NO might be further increased in activated BV2 microglia induced by LPS after exposure to iron and LiCl treatment might be decreased these productions Twenty-four hours after treatment as indicated in the figures, the levels of MMP-9, TNF-α, IL-1β and NO in the culture media of BV2 microglia were determined by gelatin zymography, ELISA and nitric oxide assay respectively. As shown in Figure 4.3, LPS significantly increased the levels of MMP-9, TNF-α, IL-1β and NO in culture media of BV2 microglia. If iron was presented during microglial activation by LPS, the levels of MMP-9 in the culture media were significantly increased without affecting the secretory levels of TNF-α. On the other hand, the present of iron significantly reduced IL-1β and NO levels in the culture media. Treatment with LiCl markedly reduced the levels of MMP-9 (A), TNF-α (B), IL-1β (C) and NO (D) in LPS-treated cultures. The presence of iron in LPS-treated cultures of BV2 microglia enhanced the inhibitory effect of LiCl only on the production of IL-1β and NO.

4.1.4 Effects of iron and LiCl on the transcription levels of inflammatory mediators, markers of microglial activation

Next, to determine whether LiCl and iron could regulate the transcription of MMP-9, TNF-α, IL-1β and iNOS mRNA. Consistent with the results obtained from

the inflammatory mediator production assay, if iron was presented during microglial activation by LPS, the transcript levels of MMP-9 were significantly increased without affecting TNF-α transcript levels (Figure 4.4A). In contrast, iron markedly decreased IL-1β and iNOS transcript levels (Figure 4.4C and D respectively). Inhibition of GSK-3β by LiCl markedly reduced transcript levels of MMP-9, TNF-α, IL-1β and iNOS in all the conditions examined. It appears that the presence of iron further enhanced the inhibitory effect of LiCl on transcript expression of IL-1β and iNOS in LPS-treated cultures of BV2 microglia. These results demonstrate that GSK-3β is involved in LPS-induced activation of BV2 microglia. Moreover, the results also demonstrate that the activation of BV2 microglia induced by LPS was modified by iron.

4.1.5 Effects of iron and LiCl on LPS-induced microglial neurotoxicity

The result in this study was demonstrated that microglial activation was modified by iron, while other studies demonstrated that microglial activation was neurotoxic to cortical, hippocampal and dopaminergic neurons. Furthermore, *in vivo* iron-enriched activated microglia have been observed along with neurodegenerative processes. Therefore the experiment was tested if iron presented during the cellular activation of microglial cells would influence microlgial neurotoxicity. In this set of experiments, the viability of neuroblastoma (NA) cells exposed to cell-free conditioned medium collected from treated cultures of BV2 microglia as indicated in the figures was determined by MTT assay. As shown in Figure 4.5A, the conditioned medium from LPS-activated microglia significantly decreased the number of NA cells. The toxicity of this medium was exacerbated if iron was present. However, the conditioned medium from iron-treated microglia alone did not affect the toxicity of NA cells. Then, the next experiment was tested if inhibition of GSK-3β would reduce the toxicity of this medium. Inhibiting GSK-3β by LiCl protected NA cells from the conditioned medium of LPS-activated microglia. The protective effect of LiCl was observed even in the presence of iron. These results demonstrated that inhibiting GSK-

3β was neuroprotective against the microglial toxicity induced by LPS. Moreover, to rule out the direct effect of iron to neurotoxicity, we also included the experiment which the BV2 microglia were treated with iron or LiCl or LPS or LPS plus LiCl or LPS plus iron or LPS plus iron and LiCl. Then, the medium were removed and replaced with fresh serum-free medium and incubated for 24 hr. After 24 hr of treatments, these conditions medium from microglial cells were collected and treated with NA cells and the neurotoxicity were assay. The result obtained from this experiment was similar to the prior experiment, as shown in figure 4.5B. Taken together, these results demonstrated that the presence of iron modified microglial activation toward a more neurotoxic effect, which could be reversed by inhibition of GSK-3β.

4.2 The effect of H63D mutation on reactive oxygen species, mitochondrial membrane potential, cytochrome c oxidase activity, GSK-3β activity, Aβ production and neuronal apoptosis

Recent evident has been reported that mutation in a gene involved in cellular iron absorption such as the HFE gene increased cellular iron uptake and increased brain iron concentration in hemocromatosis, a disorder of iron overload (Nielsen *et al.*, 1995; Berg *et al.*, 2000). Several epidemiological studies have also found an association of H63D HFE variants with AD (Sampietro *et al.*, 2001; Pulliam *et al.*, 2003; Berlin *et al.*, 2004; Connor & Lee, 2006). However, the mechanisms have not yet known. It has been reported that iron can induce oxidative stress and mitochondrial dysfunction which can cause neurodegeneration. Oxidative stress and mitochondrial dysfunction have also been observed in AD brains. Therefore, increased cellular iron uptake in cells expressing H63D HFE variant might increase oxidative stress and promote mitochondrial dysfunction which might be one mechanism that contribute to neurodegeneration.

Moreover, as in the first part, the result demonstrated that iron increased GSK-3β activity in activated microglia which appears to be enhanced microglial toxicity. Since increased GSK-3β activity has been linked to others pathology in AD including increased hyper-phosphorylation of tau protein, Aβ production as well as apoptosis. Importantly, GSK-3β activity has been reported to be increased with age (Lee *et al.*, 2006). Similar findings have also been reported for brain iron levels (Zecca *et al.*, 2004). Furthermore, the activity of GSK-3β has been shown to be elevated in AD brain (Pei et al. 1999), where iron accumulation is pronounced (Connor *et al.*, 1992a). Accordingly, increased GSK-3β activity in the normal aged brain and AD brain may be related to elevated levels of brain iron and may contribute to the pathogenesis of AD such as Aβ production and neuronal apoptosis which might be a mechanism that enhances neurodedeneration.

Therefore, the second part, neuroblastoma cell lines was used expressing H63D HFE variant to explore the mechanisms behind the associations between cellular iron status, oxidative stress, mitochondrial function, GSK-3β activity Aβ production and neuronal apoptosis which hypothesized that cells with the H63D HFE variant had a phenotype that promotes oxidative stress, mitochondrial dysfunction, GSK-3β activity, Aβ production and neuronal apoptosis.

4.2.1 Confirmation of cell transfection

The SH-SY5Y cells were chosen because they did not express detectable levels of HFE protein or mRNA (Lee *et al.*, 2007). Human neuroblastoma SH-SY5Y cell lines expressing FLAG-tagged WT and H63D forms of HFE were stably transfected as previously reported (Lee *et al.*, 2007). The protein expression of FLAG-tagged HFE was confirmed in the cells by western blotting. In addition, β-tubulin expression was also included as an internal control. As shown in Figure 4.6A, HFE protein expression can be detected following stable transfection of the SH-SY5Y cells with WT HFE and the H63D mutation while the HFE protein expression was not detected in vector

transfected cells. Because the cells transfected with vector alone do not contain HFE protein, the direct control for study the mutation of HFE, is the WT HFE transfected cells. Therefore, WT HFE cells are used as the control throughout the experiments.

4.2.2 Increased reactive oxygen species in the H63D HFE variant

Previously, it has been reported that the presence of H63D HFE allelic variant increased intracellular iron compared to cells carrying the WT HFE, consistent with the known function of the HFE protein to limit iron uptake (Lee et al. 2007b). Increased intracellular iron in the cells expressing H63D might increase the levels of reactive oxygen species in (ROS) which is major sources of oxidative stress. So, the levels of ROS in the cells expressing H63D variant were determined. The result showed significantly increased ROS in the cells expressing H63D variant comparison to cells expressing WT HFE ($p<0.05$) (Figure 4.6B).

4.2.3 Decreased the mitochondrial membrane potential in the H63D HFE variant

Increased ROS has been reported to induce lipid peroxidation resulting in alter fluidity of the inner mitochondrial membrane which might alter mitochondrial membrane potential, an important parameter of mitochondrial function. Therefore, mitochondrial membrane potential was measured in H63D cells. There was a significant decrease in mitochondrial membrane potential in the cells expressing H63D variant comparison to cells expressing WT HFE ($p<0.05$) (Figure 4.6C).

4.2.4 Reduced cytochrome c oxidase activity in the H63D cells

Decreased cytochrome c oxidase activity is a one parameter of mitochondrial dysfunction. Therefore, cytochrome c oxidase activity was also determined in the H63D cells. The result showed that significantly decreased cytochrome c oxidase activity in cells expressing H63D HFE compared to cells expressing WT HFE ($p<0.05$) (Figure 4.6D).

Taken together, these results demonstrated that increased cellular iron levels in the H63D cells leading to increased ROS and decreased markers of mitochondrial function, mitochondrial membrane potential and cytochrome c oxidase activity which might be one mechanism of iron contribute to neuronal cells death.

4.2.5 The levels of GSK-3β activity in HFE expressing cells

As in the first part, the result was demonstrated that iron increased GSK-3β activity in activated microglia, therefore, increased cellular iron levels in cells expressing H63D might increase GSK-3β activity when compared to cells expressing WT HFE. So, the next study the levels of GSK-3β activity in cells expressing H63D were determined. The activity of GSK-3β was determined by the measurement phosphorylation of GSK-3β at Ser9, a critical site known for inhibit its activity. Total cell lysates were prepared at 1 hr post-treatment and were immunoblotted with anti-phospho-Ser9-GSK-3β followed by anti-total-GSK-3β monoclonal antibodies. The levels of phospho-Ser9-GSK-3β were compared to that of total GSK-3β. As shown in Figure 4.7, the activity of GSK-3β significantly increased in cells expressing H63D compared to cells expressing WT HFE, based on decreased phosphorylation levels of GSK-3β at ser9 ($p<0.001$) .

Recently, it has also been reported that cells associated with neuritic plaques in AD express HFE and its expression is induced during exposure to stress factors including $A\beta_{25-35}$ (Lee & Connor, 2005). As the function of HFE protein is limited iron uptake. Therefore, if the mutant form of HFE is expressed during cells response to stress factors such as Aβ in AD, iron uptake may not be limited and the cell would take on more iron than normal. Therefore, if mutation of HFE is expressed during cells response to Aβ, GSK-3β activity in cells expressing H63D might be further increased. One hour after exposure of all cells to $A\beta_{25-35}$ led to increased activity of GSK-3β in all of genotypes compared to untreated cells. Importantly, the activity of GSK-3β was greater in cells expressing H63D compared to cells expressing WT HFE by $A\beta_{25-35}$

treatment ($p<0.001$) (Figure 4.7). Collectively, I demonstrated that mutation in H63D cells which lead to increase intracellular levels of iron leading to increase GSK-3β activity when compared to WT cells and that Aβ exposure further increase GSK-3β activity in H63D cells.

A growing body of evidence suggests that GSK-3β is an important modulator of apoptosis. Several studies have also shown that dying cells display the characteristics of apoptosis in AD brains and in cultures of neurons exposed to Aβ. Moreover, it has also been reported that Aβ treatment significantly increased the activity of GSK-3β follow by increased neuronal cell death through intrinsic apoptotic pathway. The previous experiment, GSK-3β was increased in H63D cells and its activity was further increased if the mutant form of HFE is expressed during cells response to Aβ. This mechanism might be factor that enhances neuronal cell death for patients who carry the mutation of HFE. Thus, the next study I pursued the main hypothesis which is the baseline increase in GSK-3β activity in H63D mutation will increased neuronal cell death which would more increase if the mutant form of HFE is expressed during cells response to Aβ.

4.2.6 Effect of $A\beta_{25-35}$ fragment on cells expressing H63D HFE compared to cells expressing WT HFE

To evaluate the viability of cells following $A\beta_{25-35}$ treatment, HFE cells were incubated with $A\beta_{25-35}$ (0, 10 or 20 μM) for 24 hr. $A\beta_{25-35}$ peptide fragment was selected because it is included in the $A\beta_{1-42}$ sequence and has been repeatedly shown to be the active toxic fragment of Aβ (Forloni *et al.*, 1993; Morais Cardoso *et al.*, 2002; Yu *et al.*, 2006). After incubation, cell viability was measured by an MTT reduction assay. In untreated cells, the viability of the cells transfected with H63D allelic variants significantly decreased compared to the cell transfected with WT HFE ($p<0.01$) (Figure 4.8A). Following $A\beta_{25-35}$ treatment, cell viability for each genotype was significantly decreased compared to untreated cells. Importantly, there was a

significantly greater decrease in the viability of the cells transfected with H63D allelic variants compared to the cell transfected with WT HFE, regardless of whether or not the cells were exposed to $A\beta_{25-35}$. In addition, $A\beta_{35-25}$, the reverse sequence of $A\beta_{25-35}$, was also included as a negative control, which did not significantly decrease cell viability in all genotypes after treatment with various concentrations (data not shown), indicating $A\beta_{25-35}$, induced its toxicity to HFE cells. The neurotoxic effect of $A\beta_{1-42}$ was also tested to compare with $A\beta_{25-35}$ exposure to verify its toxic effects as shown in figure 4.8B. Because $A\beta_{1-42}$ behaved similarly to $A\beta_{25-35}$ in inducing cells death in HFE cells, all the subsequent experiments were performed with $A\beta_{25-35}$, and because there was a significant difference between the cells transfected with H63D allelic variants and the cell transfected with WT HFE at 20 μM of both $A\beta_{25-35}$ and $A\beta_{1-42}$; 20 μM was selected as the $A\beta_{25-35}$ concentration for subsequent experiments.

4.2.7 Increased intrinsic apoptotic pathway in H63D cells compared to WT cells

To determine the effect of $A\beta_{25-35}$ on neuronal apoptosis in HFE transfected human neuroblastoma SH-SY5Y cell lines, an Annexin V-FITC/PI flow cytometry assay was performed. The cells transfected with H63D allelic variants showed slightly increased in apoptosis in basal conditions compared to the cells transfected with WT HFE. All cell types were exposed to $A\beta_{25-35}$ peptide for 24 hr and apoptosis increased across all genotypes. Importantly, there were more H63D apoptotic cells than WT HFE expressing cells ($p<0.01$) (Fig. 4.9A).

GSK-3β has been reported to enhance intrinsic apoptotic pathway by phosphorylation of Bax which lead to increase Bax translocation to mitochondria. Previous experiment, the H63D cells were demonstrated to increase GSK-3β activity compared to WT cells. Therefore, it was hypothesized that Bax translocation would be increased with H63D expression and would be further enhanced by Aβ exposure compared to WT cells. Indeed, the ratio of Bax found in the mitochondrial fraction compared to the cytosolic fraction was increased in H63D cells compared to WT HFE

cells ($p<0.001$) (Figuer 4.9B and 4.9C). After a 4 hr exposure to 20 μM $A\beta_{25-35}$, the ratio of Bax in the mitochondria to cytosol was significantly increased in all of genotypes compared to untreated cells ($p<0.001$). However, the ratio of Bax in the mitochondria to cytosol in H63D cells was also significantly increased compared to WT cells by $A\beta_{25-35}$ treatment ($p<0.001$) (Figure 4.9C). The purity of both fractions was validated by immunoblotting for marker proteins, using β-tubulin and cytochrome c oxidase subunit IV (COX) as markers for cytosol and mitochondria fractions, respectively. There was a greater than two-fold increase in the ratio of mitochondrial to cytosolic Bax in H63D cells compared to WT, regardless of whether or not the cells were exposed to $A\beta_{25-35}$

Based on enhanced Bax translocation to the mitochondria in H63D cells at baseline and upon $A\beta_{25-35}$ exposure, the next study, to evaluate cytochrome c release from the mitochondria, which is identified as an important step in promoting caspase-3 activation and hence the final phase of apoptotic cell death. Therefore, cellular fractions of the mitochondria and cytosol were obtained to evaluate cytochrome c levels among the various cell types. The data show there is greater than two-fold increase of cytochrome c release in H63D cells compared to WT cells ($p<0.001$) (Figure 4.9B and 4.9D). When the cells were treated with 20 μM $A\beta_{25-35}$ peptide to investigate the cellular response to this stress agent, there was a greater than three-fold increase of cytochrome c release in H63D cells versus WT cells ($p<0.001$) (Figure 4.9B and 4.9D).

In many apoptotic systems, mitochondrial release of cytochrome c to the cytosol interacts with and activates apoptotic protease activating factor 1 (Apaf-1). Activated Apaf-1 binds to procaspase-9, and processes them into proteolytically active forms, which subsequently initiates cleavage and activation of the executioner caspase, caspase 3. Thus, the levels of active caspase-9 and caspase-3 activity this cellular model were evaluated. There is a two-fold increase of active caspase-9 in H63D cells compared to WT cells ($p<0.001$) (Figure 4.10A). The previous experiment showed that

cytochrome c release was changed at 4 hr of $A\beta_{25-35}$ treatment. Since, caspase-9 is downstream of cytochrome c, it was expected that active caspase-9 would be changed after 4 hr of $A\beta_{25-35}$ treatment. Therefore, the cells were treated for 9 hr in order to detect caspase-9. Upon treating the cells with 20 μM $A\beta_{25-35}$ for 9 hr, levels of the active form of caspase-9 increased two-fold in cells expressing WT HFE compared to its control level, but were still at least 25% less than that seen in cells expressing H63D (Figure 4.10A). $A\beta_{25-35}$ exposure increased active caspase-9 more than 25% in cells expressing H63D compared to their baseline untreated levels.

The next study to determine caspase-3 activity, in untreated cells, caspase-3 activity was elevated in H63D cells compared to WT HFE cells ($p<0.01$) (Figure 4.10B). Subsequent, treatment of the cells with $A\beta_{25-35}$ led to an increase caspase-3 activity for all cell types compared to baseline ($p<0.01$ for WT and $p<0.001$ for H63D cells). At 8 hr of $A\beta_{25-35}$ exposure, caspase-3 activity increased in H63D cells compared to WT HFE cells ($p<0.001$) (Figure 4.10B). It also important to note that there was greater activation of caspase-3 in H63D cells upon 8 hr exposure to Aβ compared to its baseline than was seen with WT cells. Exposure for 12 hr to Aβ did not result in any additional increase in caspase-3 activity than seen at 8 hr exposure.

Caspase-8 is the key initiator of the extrinsic apoptosis signaling pathway (Nijhawan *et al.*, 2000). Thus, the levels of active caspase-8 were evaluated and found WT HFE expression to result in a 45% increase with respect to H63D expressing cells (Figure 4.10C). $A\beta_{25-35}$ treatment resulted in a decrease of active caspase-8 across all genotypes. However, in WT HFE cells, there was a 23% increase of active caspase-8 compared to H63D (Figure 4.10C).

4.2.8 Increased mitochondrial $A\beta_{1-42}$ in cells expressing H63D

In addition to neuroinflammation, increasing in oxidative stress, alterations in mitochondrial function and neuronal dying by apoptosis, abnormal accumulation of Aβ is also a critical early stage in AD neuropathology, and several studies have shown

that Aβ production is promoted by GSK-3β and reduced by GSK-3 inhibitors (Phiel *et al.*, 2003). Moreover, recent studies have found Aβ in mitochondria from postmortem brain specimens of AD patients and an accumulation of Aβ in the brain mitochondria from APP transgenic mice. Therefore, the next experiment, the Aβ production (both in cells culture medium and in mitochondria) were investigated in H63D cells compared to WT cells. The H63D allele was associated with a significant increase in mitochondrial $A\beta_{1-42}$ compared to the WT cells ($p < 0.05$) (Figure 4.11). In contrast, $A\beta_{1-42}$ in the culture medium did not change between the WT and H63D HFE alleles (Figure 4.11).

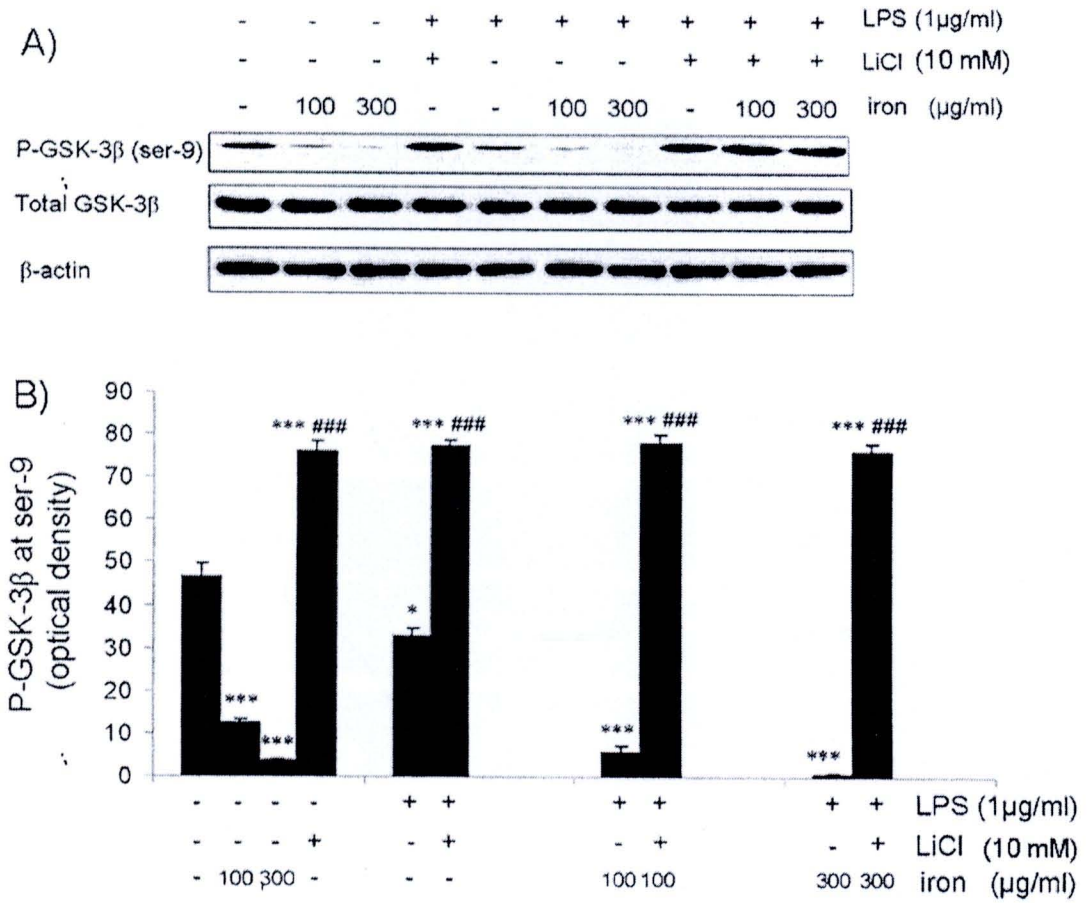

Figure 4.1 Effects of iron on inhibitory phosphorylation of GSK-3β (Ser9) in LPS-treated cultures of BV2 microglia. BV2 cells were activated by LPS and simultaneously treated with LiCl in the absence or presence of iron as indicated. After 1 hr of treatment, the levels of phospho-Ser9-GSK-3β and total GSK-3β were determined by western blot analysis as described in materials and methods. Values were expressed as mean ± SEM from three independent experiments. *p<0.05; ***p<0.001 compared to control; ###p<0.001 compared to LPS.

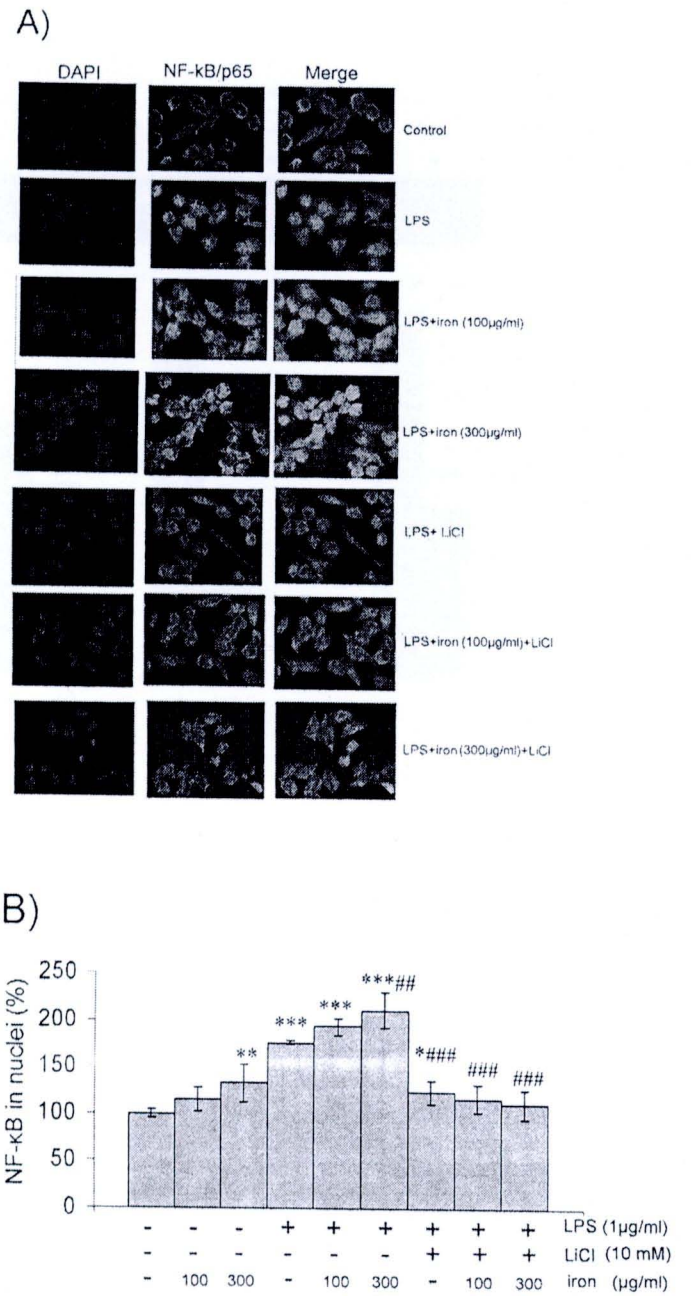

Figure 4.2 Effects of iron and LiCl on NF-κB nuclear translocation in LPS-treated cultures of BV2 microglia. BV2 cells were activated by LPS and simultaneously treated with LiCl, in the absence or presence of iron as indicated. After 4 hr of treatment, immunofluorescence staining (A) and ELISA assay (B) were performed. Values were expressed as mean ± SEM from three independent experiments. *p<0.5; **p<0.01; ***p<0.001 compared to control; ##p<0.01; ###p<0.001 compared to LPS.

A) MMP-9

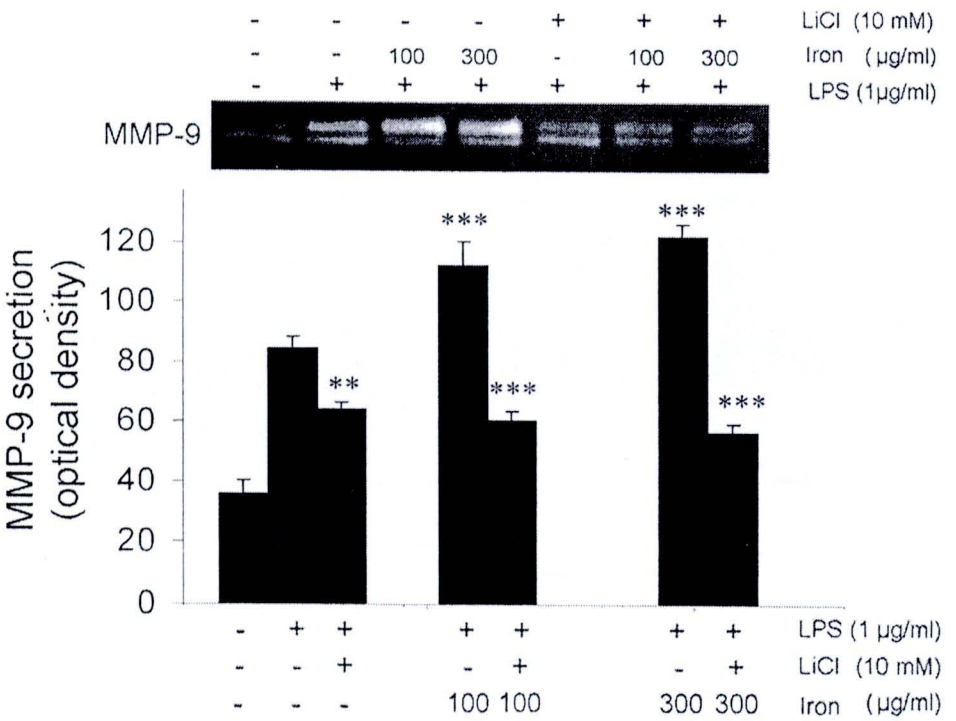
LiCl (10 mM)
Iron (μg/ml)
LPS (1μg/ml)
MMP-9
MMP-9 secretion (optical density)
120
100
80
60
40
20
0
***
**
LPS (1 μg/ml)
LiCl (10 mM)
Iron (μg/ml)
100 100
300 300

B) TNF-α

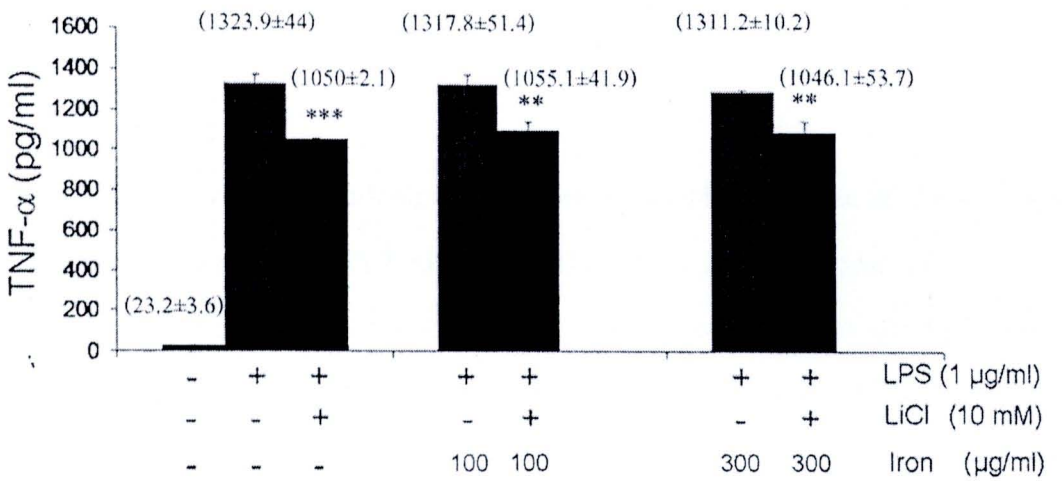
TNF-α (pg/ml)
1600
1400
1200
1000
800
600
400
200
0
(1323.9±44)
(1317.8±51.4)
(1311.2±10.2)
(1050±2.1)
(1055.1±41.9)
(1046.1±53.7)
(23.2±3.6)
***
**
LPS (1 μg/ml)
LiCl (10 mM)
Iron (μg/ml)
100 100
300 300

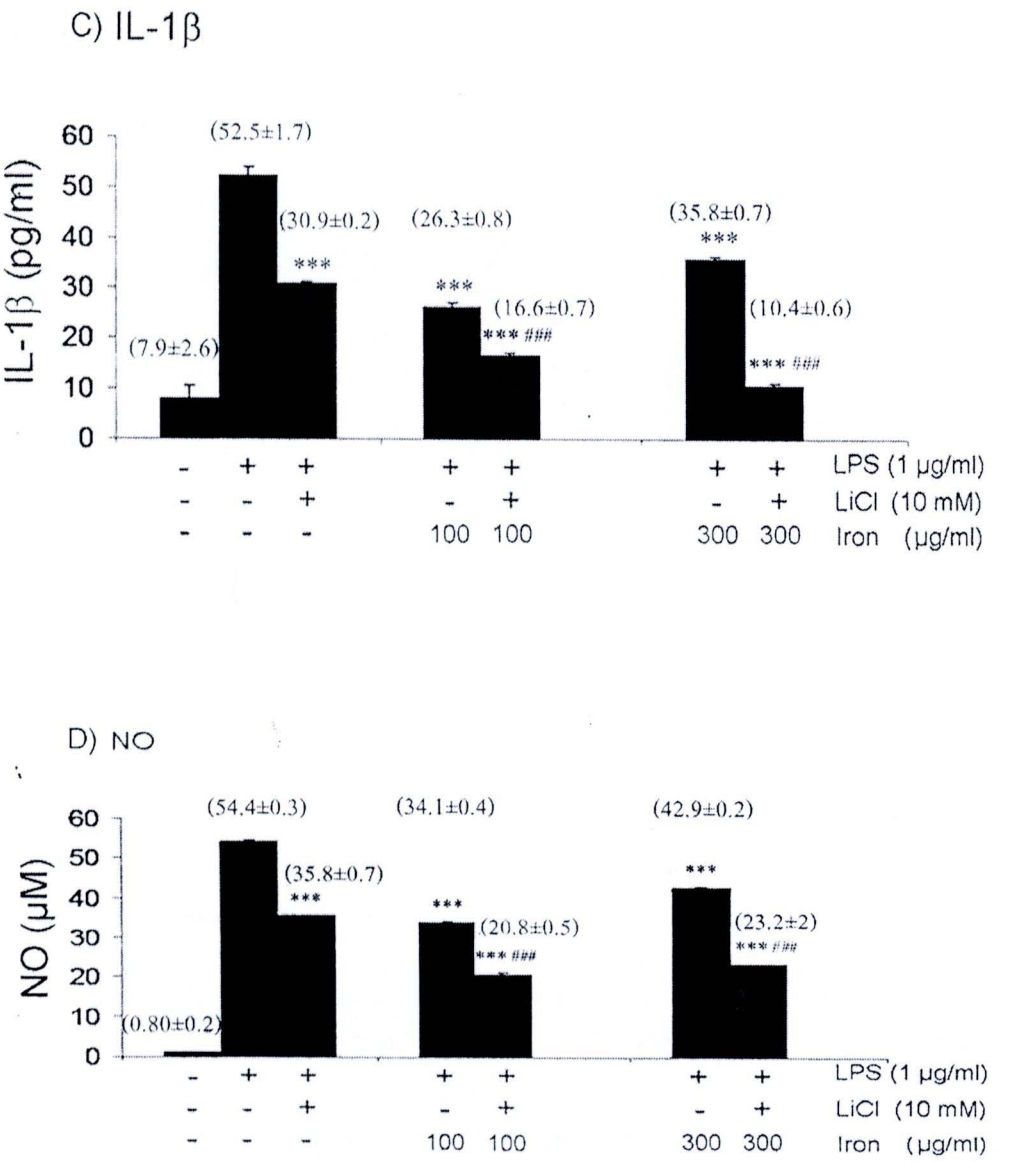

Figure 4.3 Effects of LiCl and iron on the levels of MMP-9, TNF-α, IL-1β and NO in LPS-treated cultures of BV2 microglia. BV2 cells were activated by LPS and simultaneously treated with LiCl in the absence or presence of iron as indicated. After 24 hr of treatment, the supernatants were collected and the amounts of MMP-9, TNF-α, IL-1β and NO were measured. Values were expressed as mean ± SEM from three independent experiments. **p<0.01; ***p<0.001 compared to LPS; ###p<0.001 compared to LPS+LiCl.

A) MMP-9

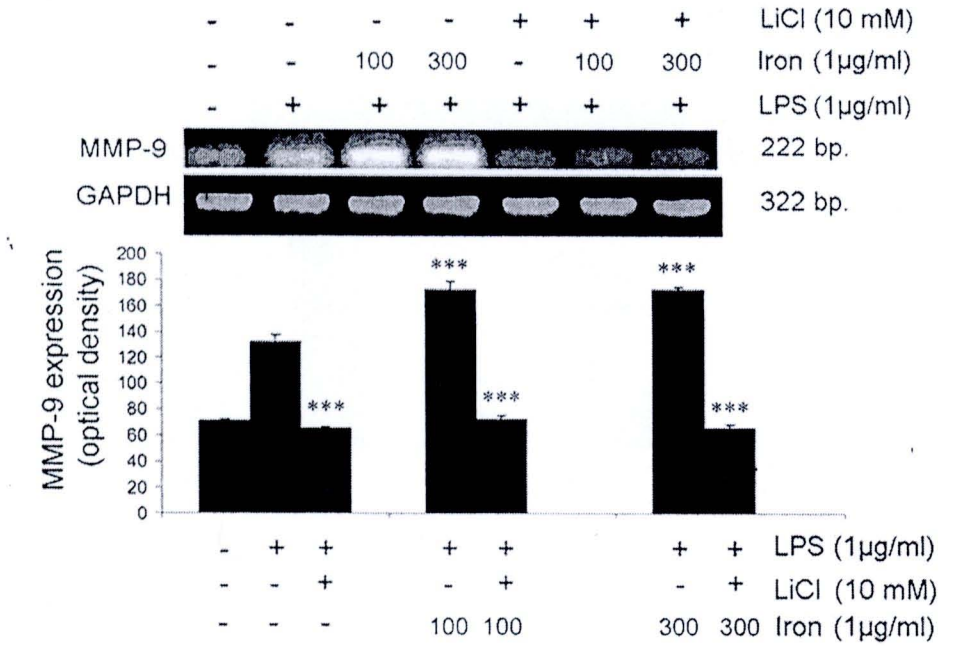
LiCl (10 mM)
Iron (1μg/ml)
LPS (1μg/ml)
MMP-9
GAPDH
222 bp.
322 bp.
MMP-9 expression (optical density)
200
180
160
140
120
100
80
60
40
20
0
***
LPS (1μg/ml)
LiCl (10 mM)
Iron (1μg/ml)

B) TNF-α

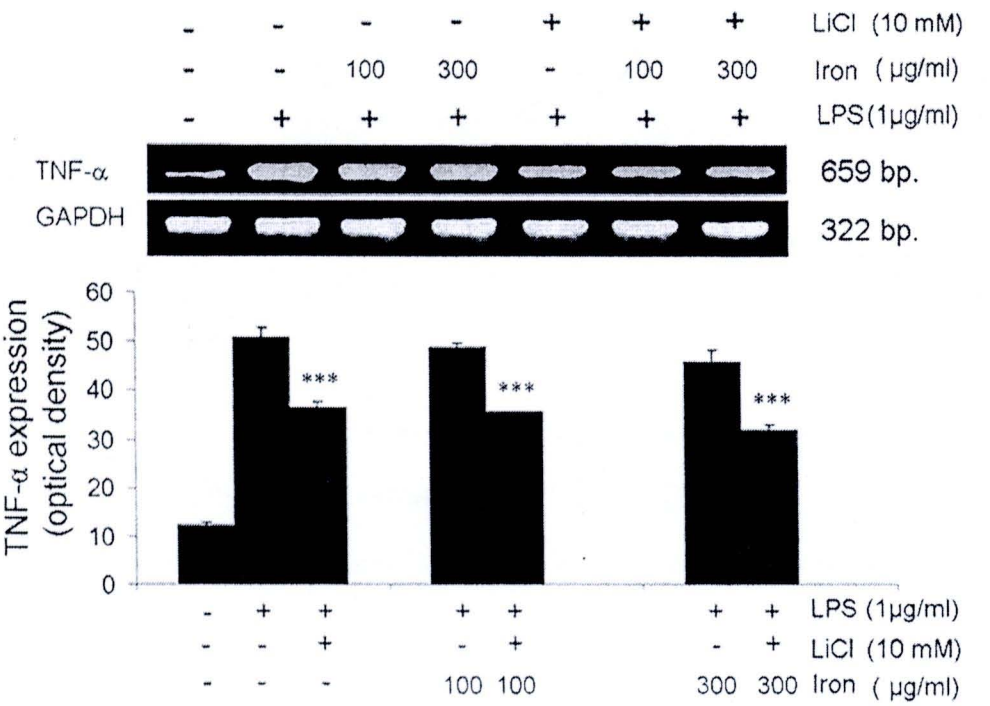
LiCl (10 mM)
Iron (μg/ml)
LPS(1μg/ml)
TNF-α
GAPDH
659 bp.
322 bp.
TNF-α expression (optical density)
60
50
40
30
20
10
0
***
LPS (1μg/ml)
LiCl (10 mM)
Iron (μg/ml)

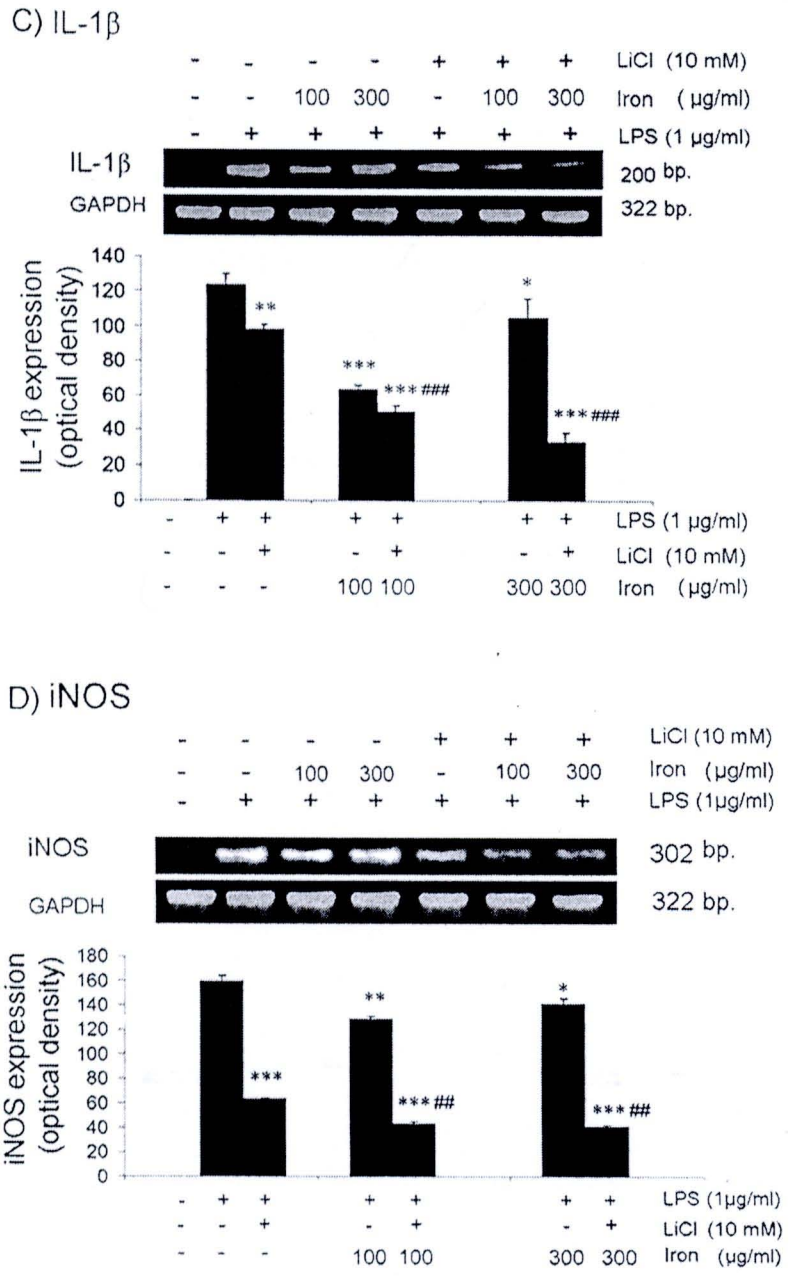

Figure 4.4 Effects of LiCl and iron on the mRNA expression of MMP-9, TNF-α, IL-1β and NO in LPS-treated cultures of BV2 microglia. BV2 cells were activated by LPS and simultaneously treated with LiCl in the absence or presence of iron as indicated. After 6 hr of treatment, the levels of MMP-9, TNF-α, IL-1β and NO mRNA were determined by RT-PCR. Values were expressed as mean ± SEM from three independent experiments. *p<0.05; **p<0.01; ***p<0.001 compared to LPS; ##p<0.01; ###p<0.001 compared to LPS+LiCl.

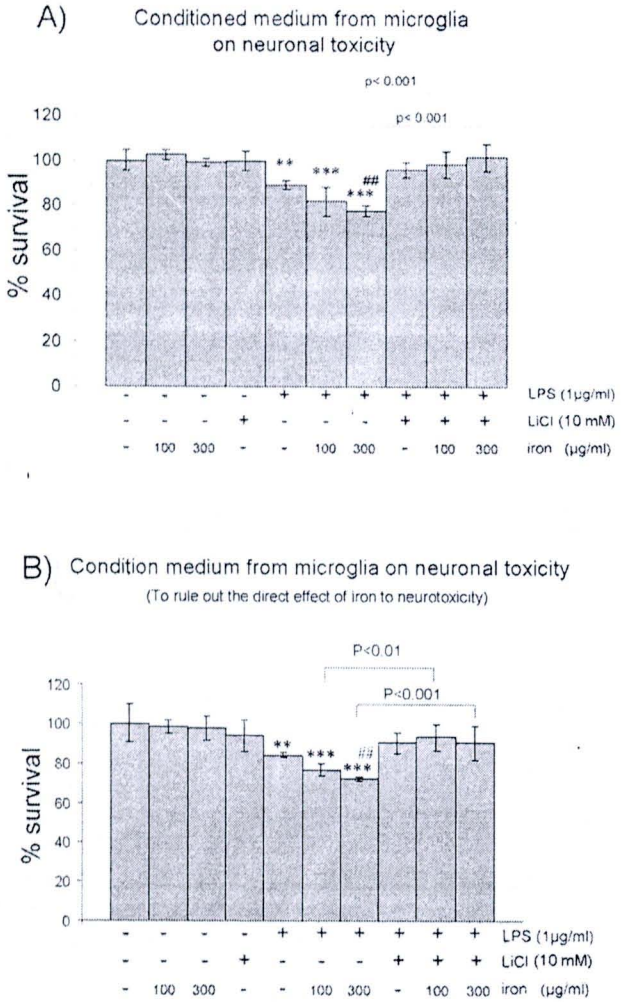

Figure 4.5 Effects of iron and LiCl on LPS-induced microglial neurotoxicity. (A) BV2 cells were activated by LPS and simultaneously treated with LiCl in the absence or presence of iron as indicated. After 24 hr of treatment, cell-free supernatants were collected and used to treat NA cells for 24 hr. After that the viability of neurons was determined by MTT assay. (B) BV2 cells were activated by LPS and simultaneously treated with LiCl in the absence or presence of iron as indicated. After 24 hr of treatment, the medium were removed and replaced with fresh serum-free medium and incubated for 24 hr. After 24 hr, cell-free supernatants were collected and used to treat NA cells for 24 hr. After that the viability of neurons was determined by MTT assay. Values were expressed as mean ± SEM from three independent experiments. **p<0.01; ***p<0.001 compared to control; ##p<0.01 compared to LPS.

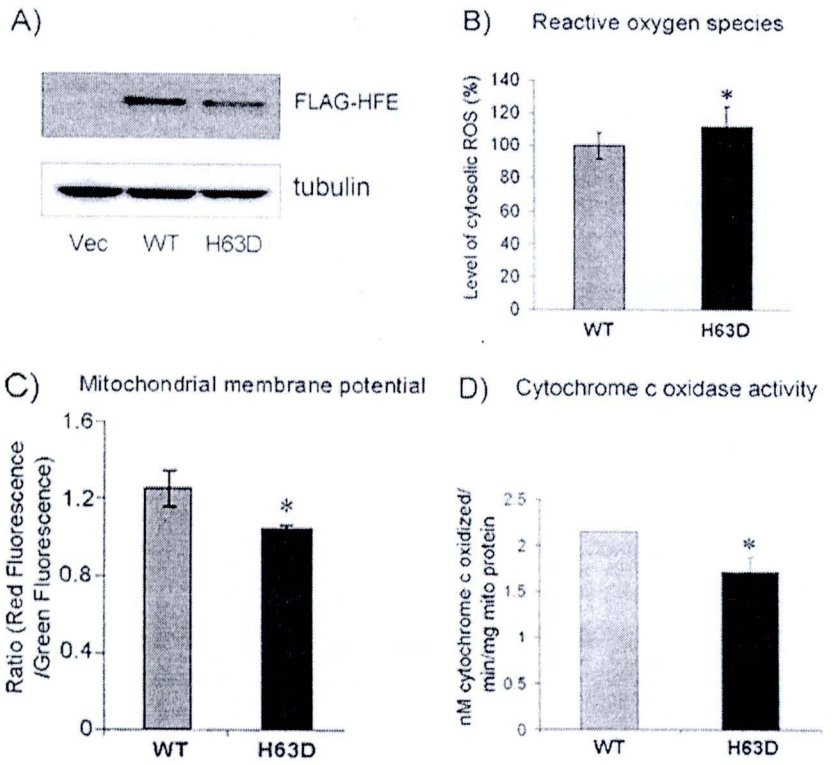

Figure 4.6 Effect of HFE variants on the oxidative stress and mitochondrial function. (A) A representative western blot is shown demonstrating FLAG-tagged HFE expression in transfected SH-SY5Y cells. (B) Increased ROS in the cells transfected with H63D allelic variants compared to the cells transfected with WT HFE. The cells were removed from growth media and resuspend cells were prewarmed in PBS buffer containing the probe as described in material and methods. (C) Decreased in mitochondrial membrane potential in the cells transfected with H63D allelic variants compared to the cells transfected with WT HFE. Mitochondrial protein was extracted from HFE cells and mitochondrial membrane potential was measured as described in material and methods. (D) Decreased cytochrome c activity in the cells transfected with H63D allelic variants compared to the cells transfected with WT HFE. Mitochondrial protein was extracted and cytochrome c activity was measured as described in material and methods. The mean represents the grand mean value obtained for each experiment.*$P<0.05$ when compared to WT; #$P<0.05$ when compared to WT treatment.

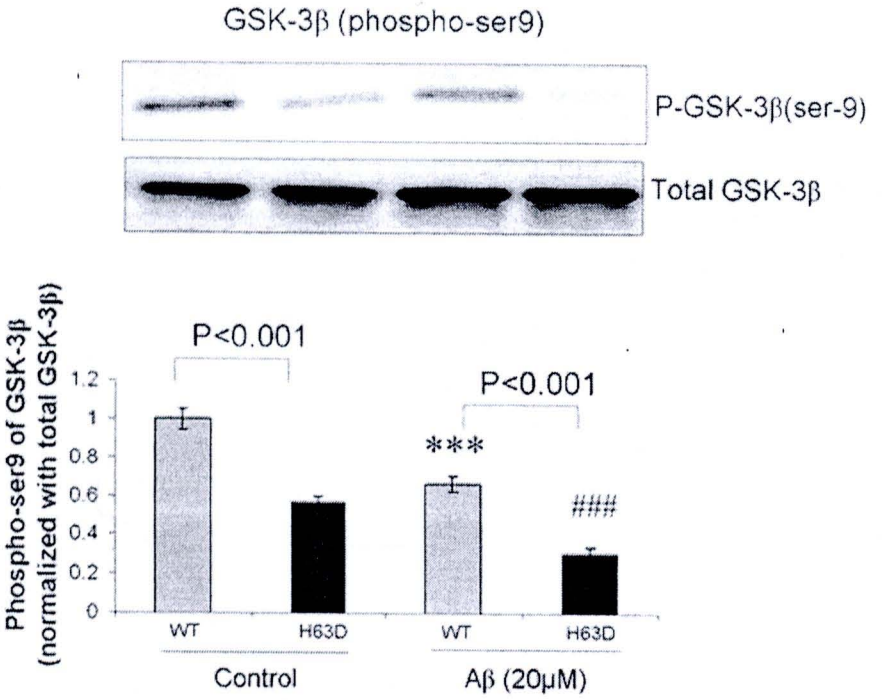

Figure 4.7 The level of phospho-Ser9 of GSK-3β in HFE expressing cells. Total cell lysates were prepared at 1 hr post-treatment and were immunoblotted for phosphorylated GSK-3β at its ser9 residue and compared to its total form. Each experiment was performed in triplicate and repeated 3 times. The mean represents the grand mean value obtained for each experiment. ***P<0.001 when compared to WT control; ###P<0.001 when compared to H63D control.

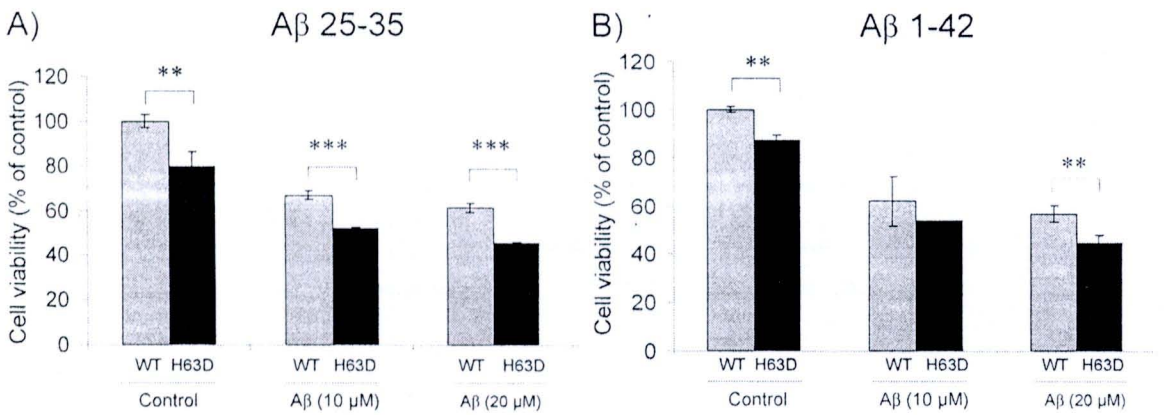

Figure 4.8 Effect of Aβ fragment ($A\beta_{25-35}$ and $A\beta_{1-42}$) on the cells transfected with H63D allelic variants compared to the cells transfected with WT HFE. HFE cells were treated with $A\beta_{25-35}$ (A) or $A\beta_{1-42}$ (B) or $A\beta_{35-25}$ (data not shown) (0, 10, or 20 μM) for 24 hr. After incubation, cell viability was measured with an MTT assay. Each experiment was performed in triplicate and repeated 3 times. The mean represents the grand mean value obtained for each experiment. **P<0.01; ***P<0.001 when compared to WT.

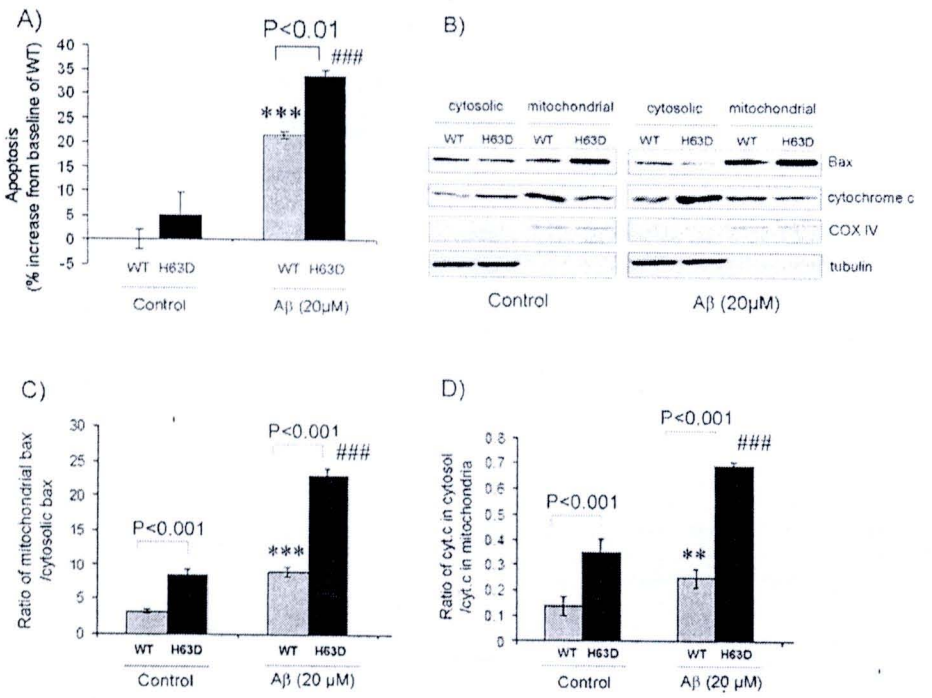

Figure 4.9 H63D cells influence basal and $A\beta_{25-35}$ induced apoptosis. (A) Cells were treated with 20 μM $A\beta_{25-35}$ for 24 hr as described in material and methods and then cells were collected and apoptosis assay were analyzed by using Annexin V-FITC/PI flow cytometry assay. (B) Cells were treated with 20 μM $A\beta_{25-35}$ for 4 hr, then the cells were fractionated to cytosolic and mitochondria-enriched fractions. Mitochondria and cytosolic fractions were immunoblotted with protein marker for each fraction, tubulin for cytosol and COX IV for mitochondria, to verify purity of fractions. The levels of Bax and cytochrome c in cytosol and mitochondria were analyzed by western blotting. (C) Densitometric analysis of the leve ls of Bax in mitochondria was normalized to the levels of COX IV (a) and the levels of Bax in cytosol was normalized to the levels of tubulin (b) (the product is the ratio between a and b). (D) Densitometric analysis of the levels of cytochrome c in cytosol was normalized to the levels of tubulin (a) and the levels of cytochrome c in mitochondria was normalized to the levels of COX IV (b) (the product is the ratio between a and b). Each experiment was performed in triplicate and repeated 3 times. The mean represents the grand mean value obtained for each experiment. **P<0.01; ***P<0.001 when compared to WT control; ###P<0.001 when compared to H63D control.

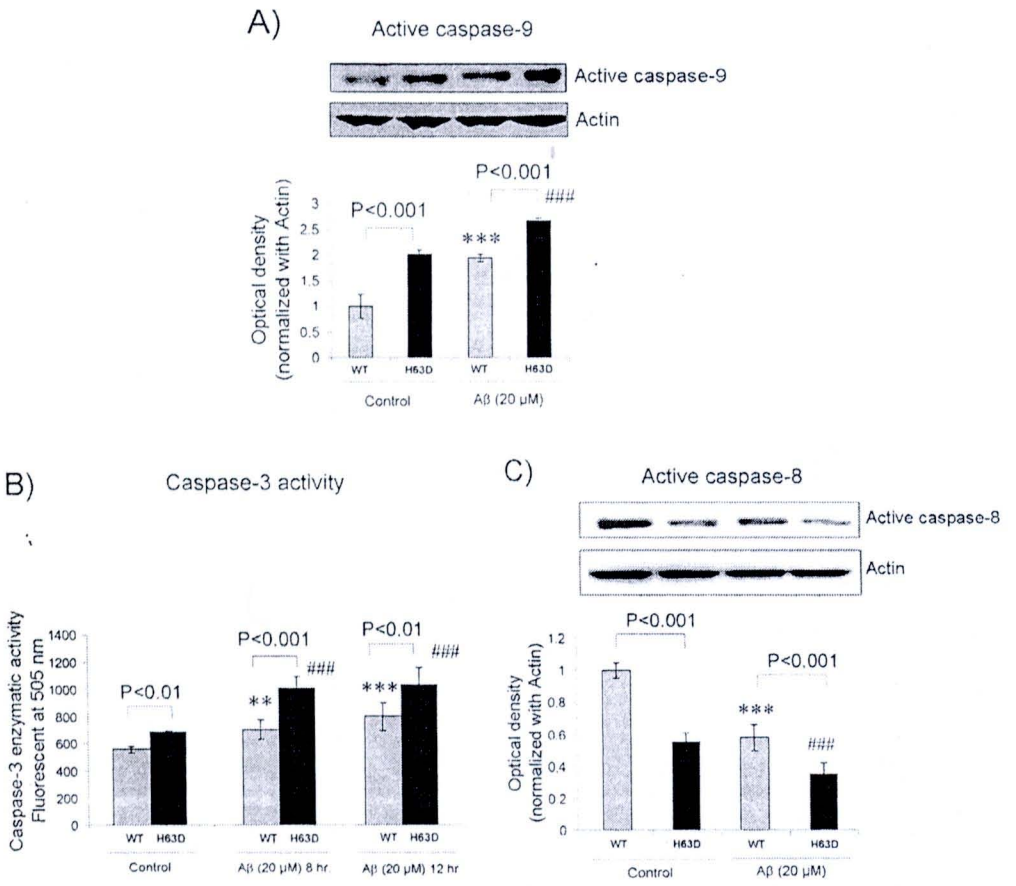

Figure 4.10 Effect of $A\beta_{25-35}$ on caspases in H63D cells. (A) Cells were treated with 20 μM $A\beta_{25-35}$ for 9 hr. Then, cells were collected and the levels of active form of caspase-9 (37 kDa) were analyzed by immunoblotting. Densitometric analysis of the levels of active caspase-9 was normalized to the levels of actin (product: actin, ratio from each treatment is further compared with WT). (B) Cells were treated for 8, and 12 hr with 20 μM of $A\beta_{25-35}$ and then cells were collected and the caspase-3 activity was determined using a caspase-3 flourometric assay. (C) Cells were treated with 20 μM $A\beta_{25-35}$ and were collected after 4 hr of treatment. Then, the levels of active form of caspase-8 (18 kDa) were analyzed by immunoblotting. Densitometric analysis of the levels of active caspase-8 was normalized to the levels of actin (product: actin, ratio from each treatment is further compared with WT). Each experiment was performed in triplicate and repeated 3 times. The mean represents the grand mean value obtained for each experiment. **P<0.01; ***P<0.001 when compared to WT control; ###P<0.001 when compared to H63D control.

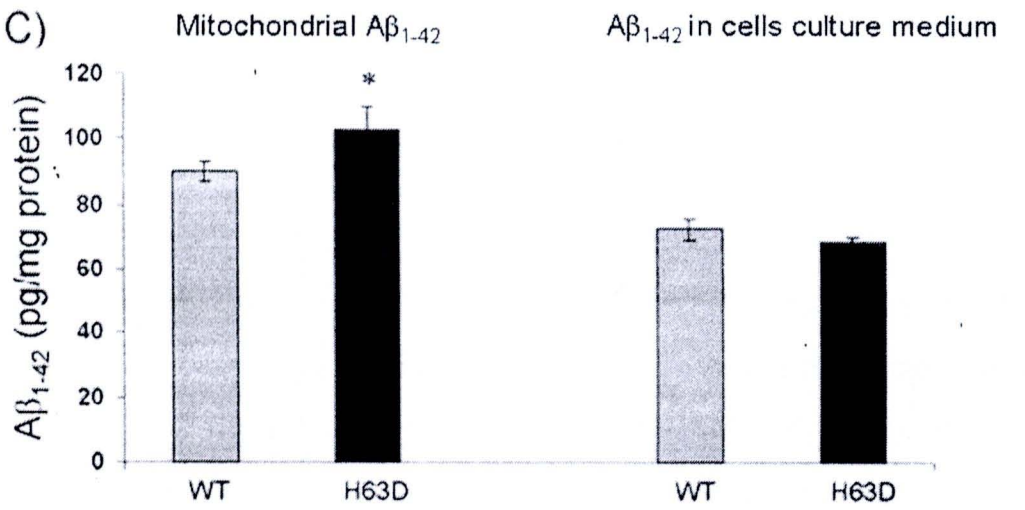

Figure 4.11 Increased levels of mitochondrial $A\beta_{1-42}$ in the H63D cells compared to WT cells. The concentration of mitochondrial $A\beta_{1-42}$ and levels of $A\beta_{1-42}$ in the culture medium was measured by ELISA using antibodies specific for $A\beta_{1-42}$. Data are shown as $A\beta_{1-42}$ pg/mg protein.Each experiment was performed in triplicate and repeated 3 times. The mean represents the grand mean value obtained for each experiment. *$P<0.05$ when compared with WT control.